Review

Bimetallic single-atom catalyst for enhancing hydrogen evolution reaction

Mengyang Zhang , Keyu Xu , Ning Sun , Yanling Zhuang , Longlu Wang * , Dafeng *Yan *

Posted Date: 8 October 2023

doi: 10.20944/preprints202310.0446.v1

Keywords: Bimetallic single-atom, Characterization, Catalytic Mechanism, Hydrogen Evolution Reaction

Review

Bimetallic Single-Atom Catalyst for Enhancing Hydrogen Evolution Reaction

Mengyang Zhang [1], Keyu Xu [1], Ning Sun [1], Yanling Zhuang [1], Longlu Wang [1,*] and Dafeng Yan [2,*]

[1] College of Electronic and Optical Engineering & College of Flexible Electronics (Future Technology), Nanjing University of Posts & Telecommunications (NJUPT),9 Wenyuan Road, Nanjing 210023, China; b22020220@njupt.edu.cn (M.Z.); b23020016@njupt.edu.cn (K.X.); b22022317@njupt.edu.cn (N.S.); zhuangyanling@njupt.edu.cn

[2] College of Chemistry and Chemical Engineering, Hubei University, Wuhan 430062, China

* Correspondence: wanglonglu@njupt.edu.cn (L.W.); dafengyan@hnu.edu.cn (D.Y.)

Abstract: Electrocatalytic and photocatalytic hydrogen evolution reaction (HER) provides a promising approach to clean energy generation. Bimetallic single-atom catalysts raised and have been explored to be advanced catalysts for HER. It is urgent to review and summarize the recent advances in developing bimetallic single-atom HER catalysts. Firstly, the fundamentals of bimetallic single-atom catalysts are presented, highlighting their unique configuration of two isolated metal atoms on supports and resultant synergistic effects. Secondly, recent advances in bimetallic single-atom catalysts for electrocatalytic HER under acidic/alkaline conditions are then reviewed, including W-Mo, Ru-Bi, Ni-Fe, Co-Ag, and other dual-atom systems on graphene and transition metal dichalcogenides (TMDs) with enhanced HER activity versus monometallic analogs due to geometric and electronic synergies. Then, Photocatalytic bimetallic single-atom catalysts on semiconducting carbon nitrides for solar H_2 production are also discussed. Finally, an outlook is provided on opportunities and challenges in precisely controlling bimetallic single-atom catalyst synthesis and gaining in-depth mechanistic insights into bimetallic interactions.

Keywords: bimetallic single-atom; characterization; catalytic mechanism; hydrogen evolution reaction

1. Introduction

Hydrogen is considered one of the most promising clean energy carriers for the future [1–4]. Catalytic water splitting provides a sustainable approach to hydrogen production using electricity from renewable resources [5]. The efficiency of the HER in the catalytic decomposition of water depends largely on the catalyst support material. Therefore, developing catalysts with optimal support interactions to reduce the energy consumption of HER has become an important focus in renewable energy research [6–11].

Single-atom catalysts, while innovative, do come with certain limitations. Their ultrafine size and isolated nature, while advantageous in some aspects, can lead to challenges [12,13]. For instance, the single-atom configuration may suffer from limited catalytic activity due to the scarcity of active sites [14–19]. Additionally, these isolated metal atoms may exhibit susceptibility to sintering, aggregation, or leaching during electrolysis, which can compromise their long-term stability and effectiveness in hydrogen production[20,21]. In contrast, bimetallic single-atom catalysts address many of these drawbacks and offer several distinct advantages [8,13] incorporating two different metal species, these catalysts harness the benefits of both single-atom and bimetallic systems. The proximity and interactions between the two distinct metal atoms in bimetallic single-atom catalysts create cooperative electronic effects and novel synergies [14,22]. This leads to enhanced catalytic activity, surpassing that of single-atom catalysts, while maintaining the stability and durability of the single-atom configuration. Furthermore, the tailored geometric and electronic structures of bimetallic single-atom catalysts allow for precise optimization of adsorption energies, reaction kinetics, and conductivity. This optimization results in improved efficiency and reliability in hydrogen production

Preprints (www.preprints.org) | NOT PEER-REVIEWED | Posted: 8 October 2023 doi:10.20944/preprints202310.0446.v1

processes. Overall, bimetallic single-atom catalysts offer a promising solution to overcome the limitations associated with single-atom catalysts, providing a path toward more efficient and stable hydrogen production [21,23,24].

In summary, bimetallic single-atom catalysts supported on 2D materials are at the forefront of developing active, robust, and inexpensive systems for clean hydrogen generation [20,25]. Further mechanistic insights into bimetallic synergies [22] and synthetic strategies to incorporate different metal pairs will be imperative to guide the rational design of optimized catalysts for hydrogen production [26,26–29]. The choice of appropriate support materials and engineering optimal catalyst-support interfaces continue to be key focuses in this emerging field.

2. The fundamentals of bimetallic single-atom catalysts for Electrocatalytic and photocatalytic Hydrogen Production

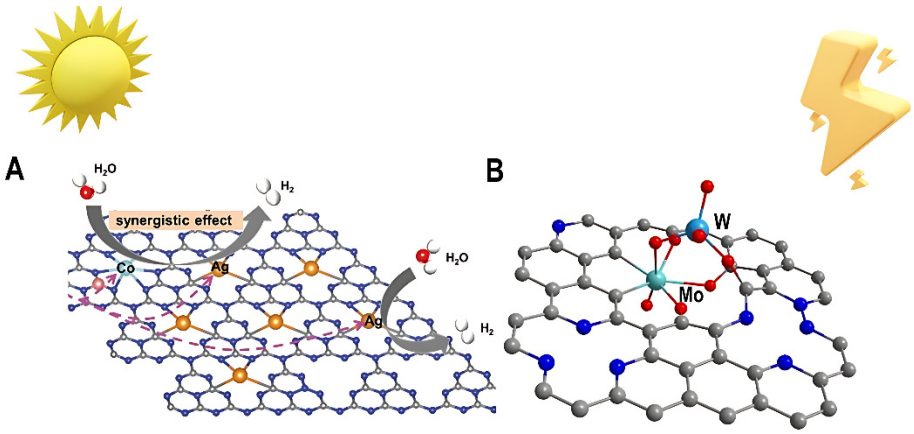

Figure 1. (A) Bimetallic single-atom catalysts for the photocatalytic generation of hydrogen Adapted with permission from [30], Copyright 2023 WILEY - V C H VERLAG GMBH & CO. KGAA; Wiley. (B) Bimetallic single-atom catalysts for electrocatalytic hydrogen production Adapted with permission from[31], Copyright 2023 American Association for the Advancement of Science.

Bimetallic single-atom catalysts have recently emerged as a promising class of electrocatalysts and photocatalysts for clean and sustainable hydrogen production. Bimetallic single-atom catalysts are composed of two different metal species anchored in close proximity as isolated atoms on a support material. The choice of support plays a critical role in determining bimetallic single-atom catalysts' performance. For electrocatalytic HER, graphene and TMDs have shown promise as versatile scaffolds. Defect engineering of these materials creates anchors to firmly immobilize the dual metal atoms [22,32,33]. For photocatalytic HER, semiconducting carbon nitrides like g-C_3N_4 provide excellent support to coordinate isolated metal atoms through their heteroatom-rich structure. This unique configuration allows bimetallic single-atom catalysts to harness synergistic effects between the two metals to optimize catalytic performance beyond their monometallic counterparts. The isolated dual metal atoms in bimetallic single-atom catalysts exhibit several advantageous features including high utilization efficiency, tunable adsorption energies, modulated electronic structure, enhanced stability, and cooperative catalysis [34–36]. With all metal atoms exposed as solitary active sites, bimetallic single-atom catalysts maximize the efficiency of the expensive noble metals [37–39]. The distinct adsorption capabilities of the two metals allow for optimizing hydrogen binding energies and intermediates activation [40–42]. The proximity interactions between the two metal atoms induce charge transfer and band structure tuning, facilitating electron transport and light absorption. Anchoring by one metal strengthens the binding of the second metal, improving thermal and chemical stability [43–45]. The two metals can selectively adsorb reactive intermediates and synergistically promote the multi-step catalytic process. These unique properties make bimetallic single-atom catalysts promising next-generation catalysts for electrocatalytic and photocatalytic HER. For photocatalytic HER, bimetallic single-atom catalysts create dual sites for redox reactions,

 doi:10.20944/preprints202310.0446.v1

promoting charge carrier separation and surface proton reduction. For electrocatalytic HER bimetallic single-atom catalysts lower the kinetic overpotentials and improve reaction rates for the critical Volmer-Heyrovsky/Volmer-Tafel steps. Overall, the tailored synergies in bimetallic single-atom catalysts stem from the proximity interactions between the two isolated metal species, which modulate the geometric and electronic environment. Further understanding of bimetallic cooperation mechanisms will be key to guiding the rational design of optimized bimetallic single-atom catalysts for efficient and durable hydrogen production across a wide pH range[22,46,47].

3. Bimetallic Single-Atom Electrocatalytic Hydrogen Production

Bimetallic single-atom electrocatalysts have shown great promise for enhancing the HER across a wide pH range. The supports for anchoring dual metal atoms play a critical role in determining the catalytic performance. Graphene and TMDs have emerged as two predominant substrates owing to their unique properties [48,49].

Graphene offers an atomically smooth surface, excellent electrical conductivity, and high carrier mobility. However, defect engineering is required to create anchors for immobilizing isolated metal atoms. Oxygen functionalization and ion bombardment have enabled graphene to firmly stabilize bimetallic atoms and achieve synergy. For instance, W and Mo heteroatoms anchored on O-sites of nitrogen-doped graphene delivered optimized HER kinetics across acidic and alkaline conditions [4,50,51].

Meanwhile, TMDs like MoS_2 provide abundant coordination sites and metallic character. Still, additional defects are needed to strengthen the interaction with single atoms. Sulfur vacancies and heteroatom doping have allowed TMDs to achieve dual-site anchoring. A combination of Ru and Ni atoms on defective MoS_2 exhibited markedly enhanced alkaline HER performance compared to single metals. The Ni substitution modulated MoS_2's electronic structure to facilitate Ru incorporation and hydrogen adsorption [52,53].

In summary, graphene and TMDs have emerged as versatile scaffolds for bimetallic single-atom electrocatalysts. Defect engineering unlocks the potential of these materials to act as supports. Ongoing research to better understand metal-substrate interactions and synergies will pave the way for rational design of optimized dual-atom electrocatalysts.

3.1. Bimetallic single-atom Catalysts Supported on Graphene

Graphene, with its hexagonal lattice structure and sp^2 hybridized orbitals, presents an atomically smooth surface lacking anchors to immobilize metal atoms. To enable graphene as a support for single-atom catalysts, the surface requires modification to create anchoring sites. Oxidative treatment is a common approach, where oxygen-containing functional groups like hydroxyl and carboxyl form on graphene through partial oxidation. These polar groups can coordinate metal atoms. Alternatively, ion bombardment can be used to induce defects in the graphene lattice, generating vacancies that trap metal atoms [20,54,55].

Modifying graphene with oxidative or ion beam treatments enables the fabrication of anchors to firmly immobilize bimetallic single atoms. This allows leveraging the conductivity and stability of pristine graphene while harnessing dual-site cooperative interactions. Further research into optimizing anchor site generation and exploring diverse bimetallic pairs on graphene holds great promise for advancing bimetallic single-atom electrocatalysis.

This paper reports the development of O-coordinated W-Mo dual-atom catalysts (DACs), W_1Mo_1-NG, for electrocatalytic HER over a wide pH range. The W_1Mo_1-NG catalyst is synthesized through a three-step hydrothermal self-assembly and chemical vapor deposition (CVD) method. In the W_1Mo_1-NG material, O-bridged W-Mo heteroatoms are inserted into the vacancies of nitrogen-doped graphene (NG) via the self-assembly of tungstate and molybdate precursors (Figure 2A). As revealed by aberration-corrected high-angle annular dark-field scanning transmission electron microscopy (AC HAADF-STEM), the distance between W-Mo atoms is below 3.6 Å (Figure 2B, 2C), markedly longer than Mo-Mo/W-Mo/W-W bonds, confirming that the W and Mo atoms are bridged by oxygen atoms. X-ray absorption fine structure (EXAFS) spectroscopy further demonstrates that

Preprints (www.preprints.org) | NOT PEER-REVIEWED | Posted: 8 October 2023 doi:10.20944/preprints202310.0446.v1

the O-bridged W-Mo heteroatoms are stabilized on NG vacancy with a W—O—Mo—O—C configuration (Figure 2D). In electrocatalytic measurements, the as-prepared W_1Mo_1-NG catalyst delivers a current density of 10 mA/cm² at an ultralow overpotential of 24 mV in 0.5 M H_2SO_4 (Figure 2E), outperforming Mo_2-NG, W_2-NG, nitrogen-doped graphene, and commercial Pt/C catalysts. Moreover, W_1Mo_1-NG exhibits an overpotential of 67 mV at 10 mA/cm² in 1.0 M KOH (Figure 2F), displaying excellent catalytic activity over a wide pH range from 0 to 14. Density functional theory calculations reveal that the delocalized electrons in the distinctive W—O—Mo—O—C configuration provide near-optimal hydrogen binding energy, facilitating superior HER kinetics (Figure 2G) After continuous electrolysis for 80,000 seconds at 10 mA/cm², W_1Mo_1-NG retains 98% and 95% of its initial overpotential in acidic and alkaline media, respectively (Figure 2H), manifesting outstanding stability. The synergistic effect and electronic structure modulation of the W-Mo dual atoms in W_1Mo_1-NG is crucial for the high catalytic activity and stability over the entire pH range.

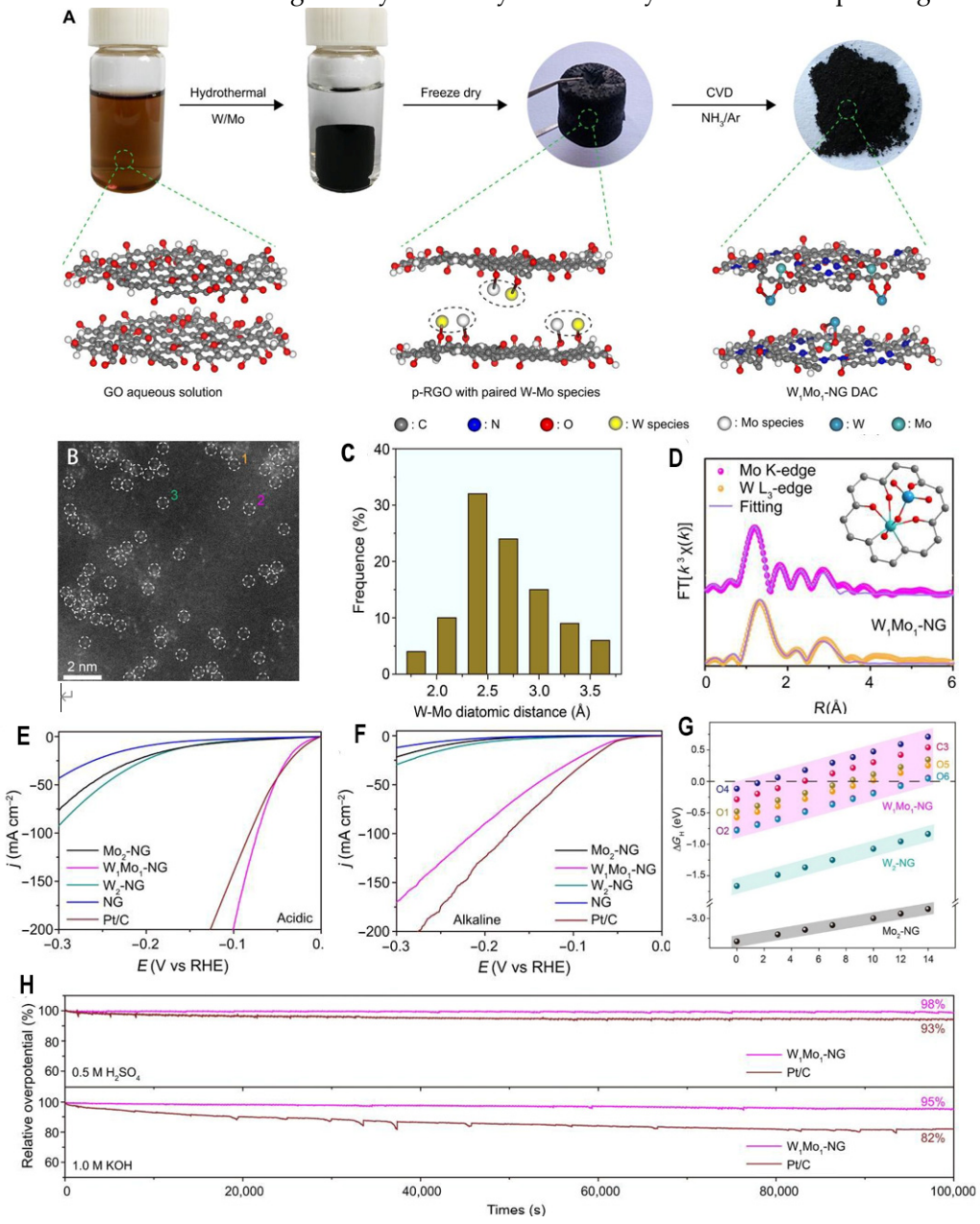

Figure 2. (A) Schematic illustration of the synthetic procedure. (B) AC HAADF-STEM images. This image shows paired W-Mo atoms. (white circles). (C) The distance between statistical W-Mo diatomic in AC HAADF-STEM images. (D) The corresponding Mo K-edge and W L_3-edge EXAFS fitting curves for W_1Mo_1-NG at R-space. (E and F) The polarization curves of Mo_2-NG, W_1Mo_1-NG, W_2-NG, NG, and Pt/C were measured in 0.5 M H_2SO_4 and 1.0 M KOH. (G) ΔG_H diagrams of W_1Mo_1-NG, Mo_2-NG,

 doi:10.20944/preprints202310.0446.v1

and W_2-NG. The differential charge density maps of heteronuclear W_1Mo_1-NG system (H) Galvanostatic responses of W_1Mo_1-NG and Pt/C were recorded at 10 mA cm^{-2} under acidic and alkaline solutions. Adapted with permission from[31], Copyright 2023 American Association for the Advancement of Science.

The paper reported an efficient alkaline HER electrocatalyst composed of RuBi single-atom alloy (SAA) decorated on Bi-single-atom-doped oxidized graphene (RuBi SAA/Bi@OG) (Figure 3A). This novel nanostructure was successfully synthesized via a facile pyrolysis approach. Morphological characterizations by transmission electron microscopy (TEM) (Figure 3B) demonstrate the uniform distribution of RuBi SAA nanoparticles on the OG substrate. The high-resolution TEM and selected area electron diffraction patterns confirm the dominant exposure of the Ru crystal facet in RuBi SAA. More importantly, as displayed in the element mapping results in Figure 3C, the Ru and Bi elements are homogeneously distributed in the RuBi SAA/Bi@OG sample, confirming the dual positioning of Bi and Ru atoms. X-ray absorption spectroscopy (XAS) provides critical structural insights. The Ru K-edge and Bi L_3-edge XANES spectra verify the metallic nature of Ru and the lower oxidization state of Bi in Rubi SAA/Bi@OG, respectively (Figure 3D,3E). No characteristic Bi-Bi peak is observed in FT-EXAFS (Figure 3E), demonstrating the isolated single-atom feature of Bi. These results strongly validate the proposed dual-positioning of Bi single atoms in the RuBi SAA and OG support. Owing to the modulated electronic structure, Rubi SAA/Bi@OG delivers substantially enhanced alkaline HER performance relative to Ru NP/OG and Pt/C (Figure 3F, 3G). At an overpotential of 150 mV, its exceptional mass activity reaches 65,000 mA mg^{-1}, which is 72.2 and 3.6 times higher than commercial Pt/C and Ru NP/OG, respectively (Figure 3F). DFT calculations reveal the Rubi SAA/Bi@OG nanostructure possesses the optimal hydrogen adsorption free energy on Ru sites (-0.37 eV), benefiting from the double atomic tuning effect (Figure 3H).

Preprints (www.preprints.org) | NOT PEER-REVIEWED | Posted: 8 October 2023 doi:10.20944/preprints202310.0446.v1

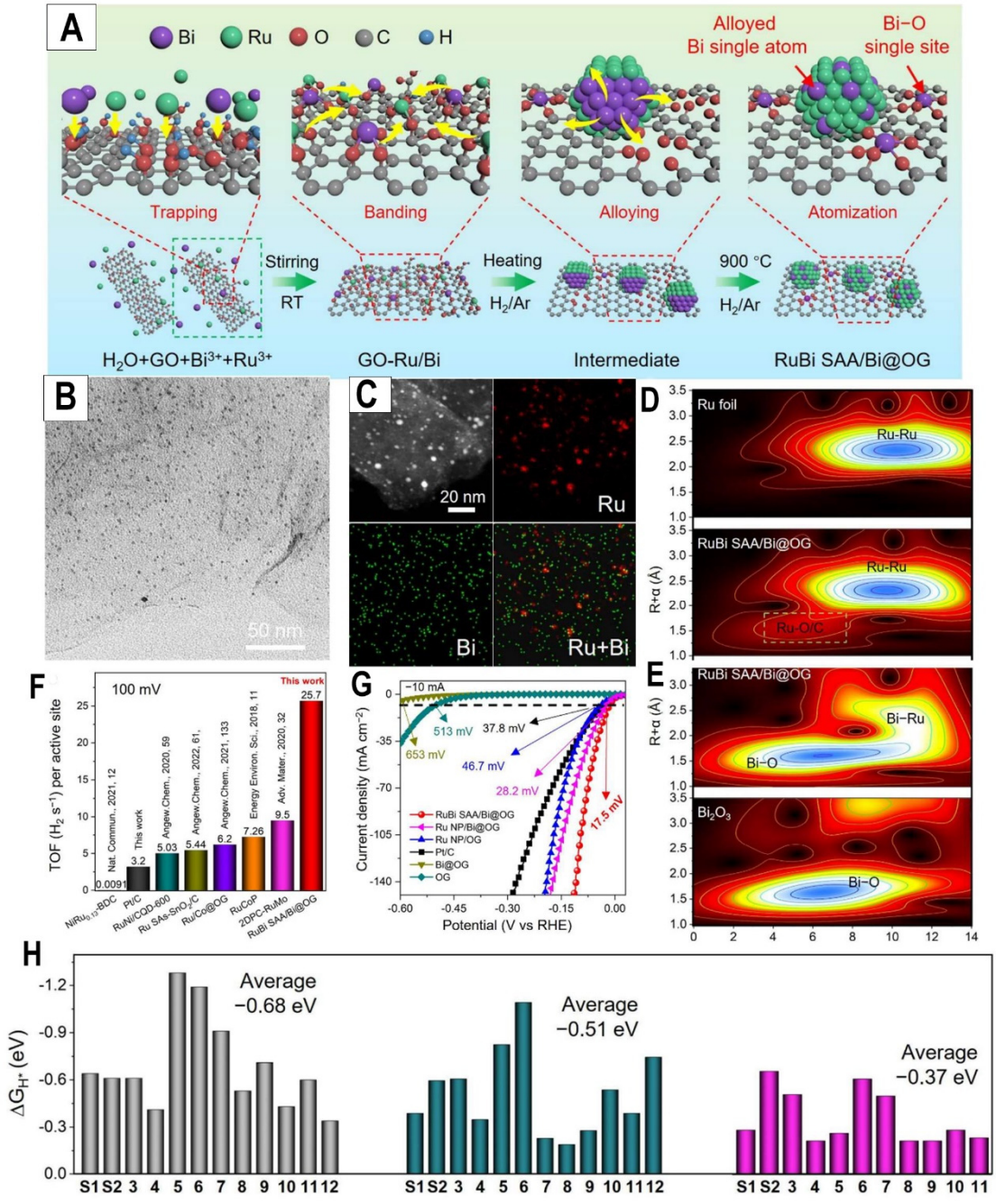

Figure 3. (A) Schematic illustration for preparation of RuBi SAA/Bi@OG (B) TEM. (C) The Ru and Bi elements in the RuBi SAA/Bi@OG were mapped using EDS. (D) The K_3-weighted EXAFS signals of Ru foil, RuBi SAA/Bi@OG, and RuO_2 were analyzed using wavelet transforms. (E) The wavelet transforms for the K_3 -weighted EXAFS signals of Bi foil, RuBi SAA/Bi@OG, and Bi_2O_3. (F) The mass-specific activity at an overpotential of 50, 100, and 150 mV. (G) Comparison of TOF values of state-of-the-art Ru-based alloy HER electrocatalysts at an overpotential of 100 mV. (H) Calculated hydrogen-adsorption Gibbs free energy (ΔG_{H^*}) of different adsorption sites in Ru_{13}/O_6G, $Ru_{13}/Bi_1@O6G$ and $Ru_{12}Bi_1/Bi1@O_6G$, respectively. Adapted with permission from [56], Copyright 2023 ANGEWANDTE CHEMIE.

3.2. Bimetallic Single-Atom Catalysts Supported on TMDs

Preprints (www.preprints.org) | NOT PEER-REVIEWED | Posted: 8 October 2023 doi:10.20944/preprints202310.0446.v1

TMDs like MoS_2 have emerged as promising supports for bimetallic single-atom catalysts, owing to their metallic character, high conductivity, and abundance of unsaturated coordination sites [57–59]. However, pristine TMD surfaces lack sufficient anchoring sites to firmly immobilize isolated metal atoms. Similar to graphene, creating defects in the lattice structure of TMDs has proven an effective approach for engineering stable anchors. For example, sulfur vacancies in the MoS_2 basal plane can coordinate single metal atoms through strong bonding with the exposed Mo atoms. Alternatively, heteroatom doping, such as partially replacing Mo with Ni or Co, can also modulate the TMD electronic structure and generate additional low-coordination sites [60–64].

In summary, creating sulfur vacancies and heteroatom doping enables TMDs to firmly stabilize isolated bimetallic atoms. Further research into defect control and TMD compositional tuning will open up new possibilities for designing optimized TMD-supported single-atom catalysts.

Recent advances in single-atom catalysts have shown great promise for electrochemical reactions like the HER However, stability and activity limitations persist for single-metal systems. Ge et al. report a bimetallic single-atom catalyst composed of Ru and Ni anchored on MoS_2 nanosheets (Ru/Ni-MoS_2) (Figure 4A, 4B, 4C) that exhibits excellent HER performance and durability.

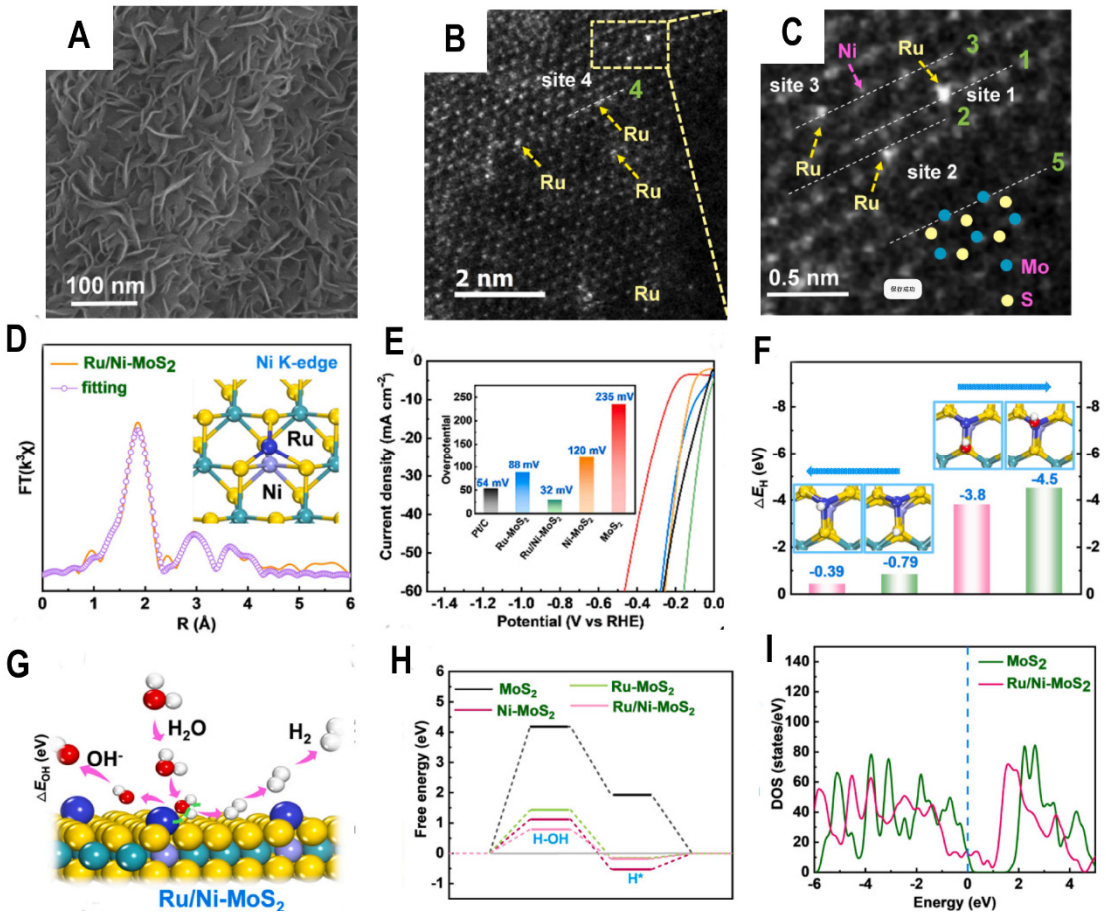

Figure 4. (A) SEM image of Ru/Ni-MoS_2/CFP. (B) The HAADF-STEM image and (C) corresponding enlarged image of Ru/Ni-MoS_2. (D) EXAFS fitting curves of Ni K-edge in Ru/Ni-MoS_2 (insets: atomic structure model of Ru/Ni-MoS_2). (E) The LSV curves of CFP, MoS_2/CFP, Ni-MoS_2/CFP, Ru-MoS_2/CFP, Ru/Ni-MoS_2/CFP and 5 wt.% Pt/C without IR correction (Inset: overpotential (η10) of these samples). (F) DFT-calculated adsorption energies of H and OH at different positions on the surfaces of Ru/Ni-MoS_2, respectively. (G) The illustration of the mechanism for the electrocatalytic HER under alkaline conditions. (H) Free energy diagrams on the surface of these catalysts in an alkaline solution. (I) The calculated DOS of pristine MoS_2 and Ru/Ni-MoS_2. Adapted with permission from[53], Copyright 2021 ELSEVIER BV.

Using a combination of microscopy, spectroscopy, and computations, they confirm that Ru atoms are primarily bonded through Ni atoms substituting Mo sites in the MoS_2 lattice (Figure 4D).

 doi:10.20944/preprints202310.0446.v1

The strong electronegativity of Ni facilitates electron transfer to the MoS_2 support and stable incorporation of Ru. Electrochemical testing reveals the Ru/Ni-MoS_2 catalyst has an ultralow overpotential of 32 mV and Tafel slope of 41 mV/dec (Figure 4E), significantly outperforming MoS_2, Ru/MoS_2, and Ni/MoS_2. DFT calculations suggest a synergistic effect where Ni-bonded S sites adsorb H while Ru sites bind OH, together accelerating the water dissociation step crucial for alkaline HER (Figure 4F). DFT calculations also elucidate how Ni substitution enables Ru incorporation and modulates MoS_2's electronic structure (Figure 4G). Ni atoms replacing Mo are energetically favorable and lead to electron accumulation on neighboring S sites. This increases S affinity for hydrogen and promotes charge transfer from Ru atoms. The modulated electronic structure is central to achieving the high HER activity of Ru/Ni-MoS_2. The alkaline HER mechanism involves water adsorption, dissociation, and hydrogen generation steps. Ge et al. constructed free energy diagrams to gain insights into how Ru/Ni-MoS_2 promotes this process (Figure 4H). Compared to MoS_2, Ru-MoS_2, and Ni-MoS_2, Ru/Ni-MoS_2 has the lowest hydrogen adsorption free energy, facilitating hydrogen evolution. More importantly, the water dissociation barrier is significantly reduced on Ru/Ni-MoS_2 due to the synergistic adsorption of hydrogen and hydroxide discussed earlier. Furthermore, the bimetallic single-atom structure enhances conductivity by narrowing the bandgap of MoS_2 (Figure 4I), while the Ni anchoring minimizes Ru leaching to give remarkable 20-hour stability.

Overall, this rational design of a bimetallic single-atom catalyst utilizing heteroatom electronegativity differences provides a promising strategy for developing highly active and stable HER electrocatalysts. The novel insights into controlling metal-support interactions and catalytic mechanisms will inform further advances in this emerging field.

The development of highly efficient and stable electrocatalysts for acidic overall water splitting is of great importance for sustainable hydrogen production but remains a huge challenge. (Figure 5A) Recently, Jiang et al. proposed an ingenious approach to assemble diatomic species (DAs) of Ni and Fe into the interlayer of MoS_2. This interlayer-confined NiFe@MoS_2 structure was synthesized via laser molecular beam epitaxy and subsequent self-curving treatment. (Figure 5B) Aberration-corrected scanning transmission electron microscopy (STEM) directly revealed the atomic configuration of Ni and Fe DAs anchored at sulfur vacancies within the MoS_2 interlayer. (Figure 5C) Compared to pristine MoS_2, electron spin resonance spectra confirmed the anchoring of NiFe DAs at sulfur vacancies in planar NiFe@MoS_2. (Figure 5D) Density functional theory calculations demonstrated the interlayer confinement effect optimized the hydrogen and oxygen adsorption capability and reduced the energy barriers, thereby facilitating acidic overall water splitting. (Figure 5E-G) Impressively, it achieved ultra-efficient acidic overall water splitting with superb durability. (Figure 5H 5I) Experimentally, the interlayer-confined NiFe@MoS_2 exhibited enhanced HER and oxygen evolution reaction (OER) activities.

Preprints (www.preprints.org) | NOT PEER-REVIEWED | Posted: 8 October 2023 doi:10.20944/preprints202310.0446.v1

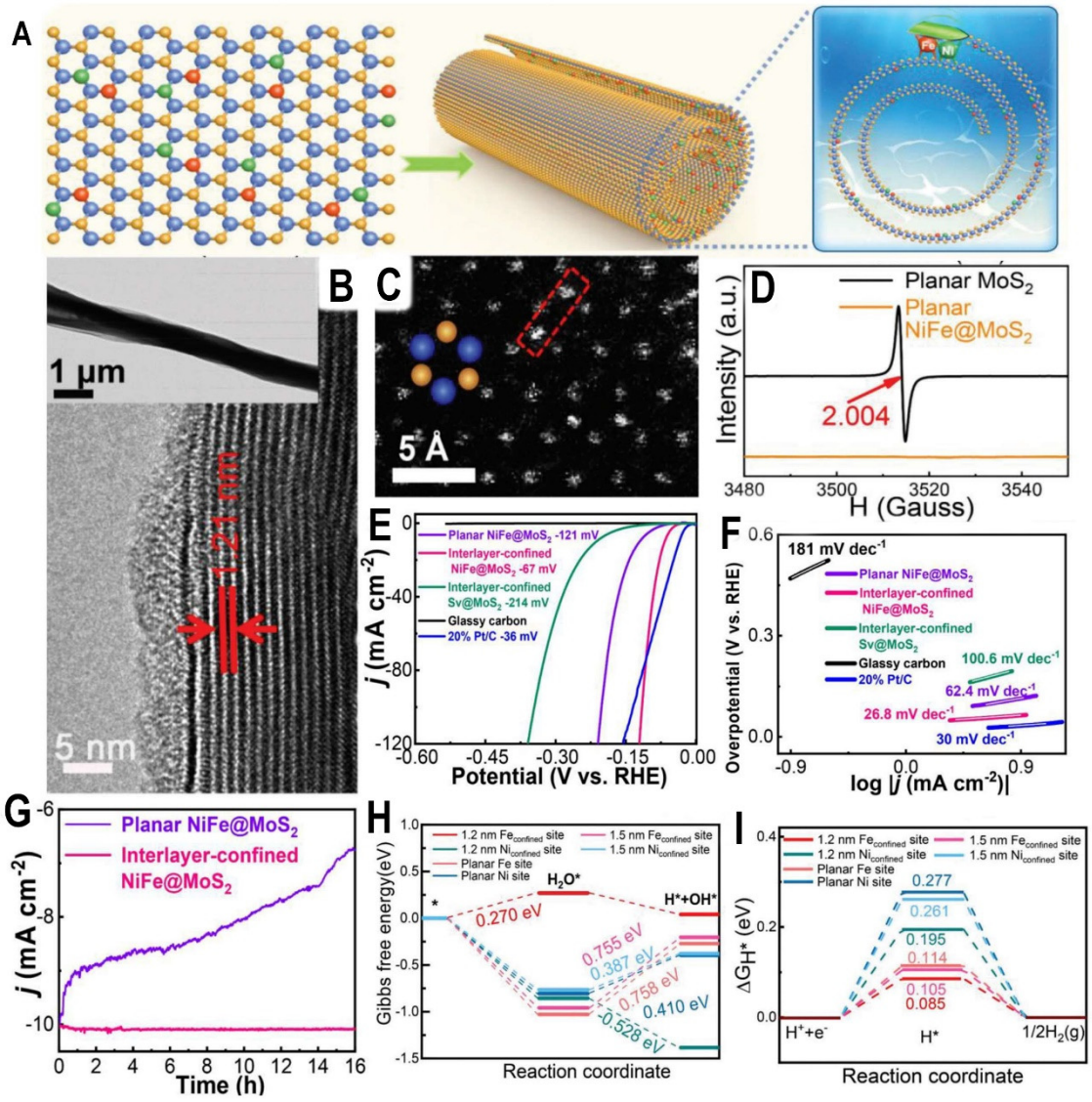

Figure 5. (A) The proposal aims to assemble DAs with atomic-scale precision in adjacent layers within the 2D limit. (B) HAADF-STEM of sidewalls of interlayer-confined NiFe@MoS_2, inset is the corresponding low-magnification TEM image. (C) An atomic-resolution aberration-corrected HAADF-STEM image is shown, with Mo and S represented by blue and orange balls, respectively, in interlayer-confined NiFe@MoS_2. (D) ESR spectra of pristine monolayer MoS_2 and planar NiFe@MoS_2. (E) Polarization curves and (F) Tafel plots of interlayer-confined NiFe@MoS_2, planar NiFe@MoS_2, interlayer-confined Sv@MoS_2, bare glassy carbon electrodes and 20% Pt/C for HER. (G) Amperometric j–t tests of interlayer-confined NiFe@MoS_2 and planar NiFe@MoS_2. (H) Water dissociation barrier comparison. (I) Standard free energy diagram of the HER process Adapted with permission from[65], Copyright 2023 Wiley-VCH.

This work embodies the significance of interlayer confinement in regulating the adsorption properties and stabilizing the highly active dual atoms even in harsh conditions. The atomic-level spatial restriction provides a protective "shelter" for the dual atoms to survive acidic electrolytes. Moreover, this general confinement approach based on 2D materials interlayer allows the incorporation of various active species, which opens up possibilities for designing advanced interlayer-confined electrocatalysts for diverse energy-related applications. In summary, the atomic-scale interlayer-confinement of multiple species represents a promising strategy to develop optimized and robust catalytic systems with both high efficiency and durability. Further exploitation

 doi:10.20944/preprints202310.0446.v1

of such confined configurations and the confinement effects may provide valuable insights into rational catalyst design

4. Bimetallic single-atom Photocatalysts for Hydrogen Production

Semiconducting carbon nitrides, including phosphorus-doped carbon nitride (PCN) and two-dimensional polymerized carbon nitride (2D CN), have attracted great interest as metal-free photocatalysts for solar-driven hydrogen production. However, rapid recombination of photogenerated charge carriers remains a key limitation. Anchoring isolated dual metal atoms on the carbon nitride surface creates catalytic sites to facilitate charge separation and surface redox reactions.[14,41,66–68]. The conjugate structure of carbon nitrides with delocalized π electrons enables strong coordination with metal atoms through the electron-rich nitrogen sites. Studies have shown that single atoms of Pt, Co, and Ag can be stably incorporated into the heptazine units of the carbon nitride lattice. The dual metal atoms act as electron trapping sites, spatially separating the photogenerated electrons and holes [69–73].

In summary, carbon nitride semiconductors provide versatile scaffolds for stabilizing bimetallic single-atom photocatalysts. The heteroatom-rich structure firmly anchors isolated metal atoms to create dual-site systems with tunable properties and synergistic effects. Further research into synthetic control and mechanistic elucidation will advance the development of efficient carbon nitride-based photocatalysts.

4.1. Bimetallic single-atom Catalysts Supported on Phosphorus-Doped Carbon Nitride

Photocatalytic water splitting for hydrogen production using solar energy has attracted tremendous attention. Single-atom catalysts (SACs) have been developed to maximize atom utilization efficiency. However, the catalytic activity of mono-metallic SACs is still limited due to insufficient active sites. Constructing dual-atom catalysts (DACs) by incorporation of a second metal has proven an effective approach to achieve cooperative effects between dual metal sites. Recently, Liu et al. reported double-metal SACs with Co and Ag anchored on phosphorus-doped carbon nitride (PCN) sheets using supramolecular and solvothermal methods

Figure 6A presents the proposed mechanism that the Co-Ag dual sites act as electron sinks for photogenerated electrons while the remaining holes oxidize water. This Co_1Ag_1-PCN DAC exhibited remarkably enhanced photocatalytic hydrogen evolution from water splitting under simulated sunlight, achieving an impressive H_2 production rate of 1190 μmol g^{-1} h^{-1} (Figure 6B). In contrast, the incorporation of Ag or Co alone only led to moderate improvement over PCN. Figure 6C presents the high apparent quantum efficiency (AQY) of 1.49% at 365 nm, consistent with the enhanced light harvesting capability. (Figure 6D) shows the excellent stability of Co_1Ag_1-PCN over multiple cycles. (Figure 6E) presents the Mott-Schottky plots, suggesting the optimized band structure of Co_1Ag_1-PCN. The partial density of states calculated by DFT (Figure 6F, 6G) shows the band center shift closer to the Fermi level for the dual metal sites. Density functional theory calculations illustrate the modulated electronic structure and synergistic effects between the dual-metal centers (Figure 6H). The integration of Co redistributes the charge density surrounding Ag atoms, facilitating interfacial charge transfer.

Preprints (www.preprints.org) | NOT PEER-REVIEWED | Posted: 8 October 2023 doi:10.20944/preprints202310.0446.v1

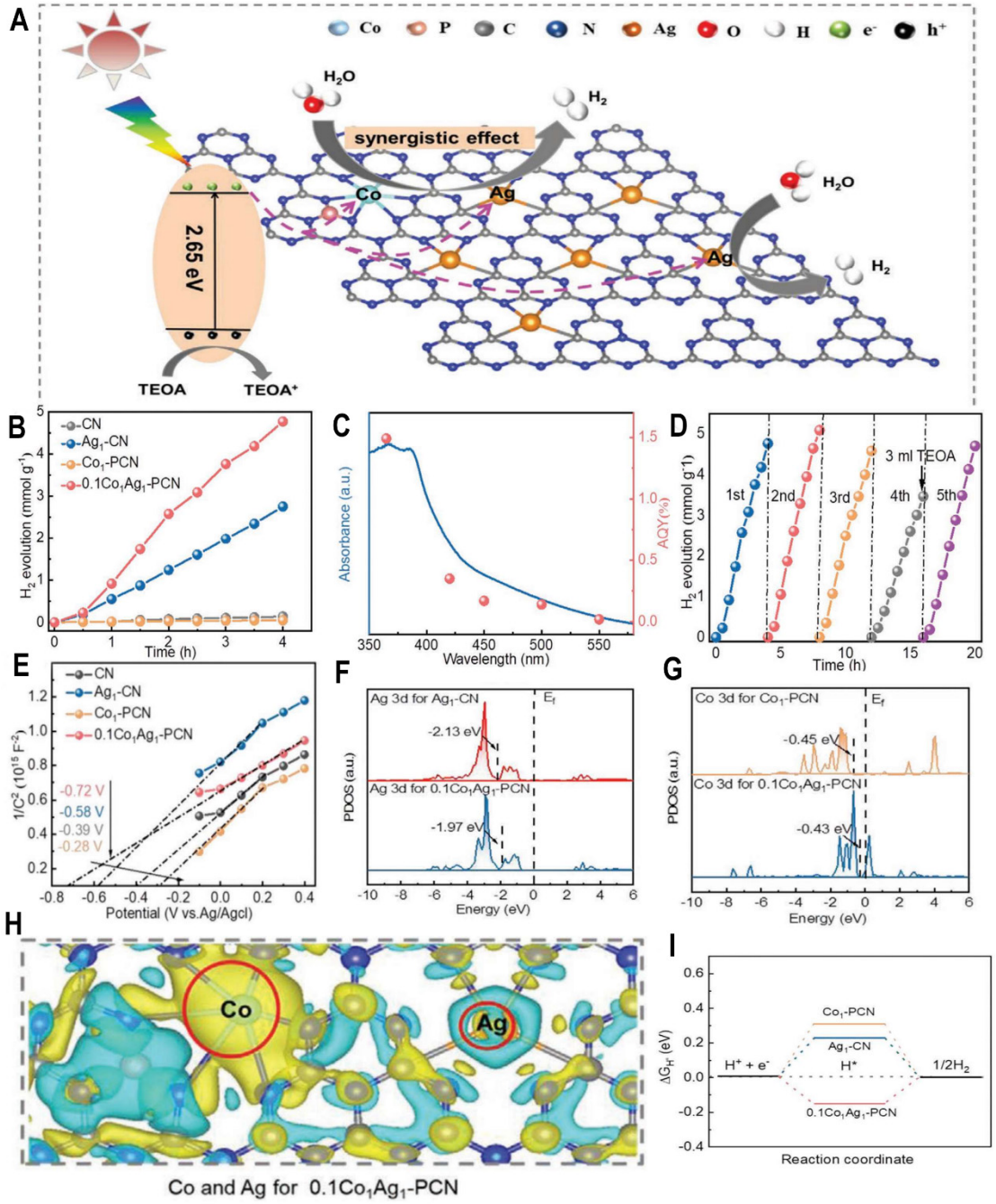

Figure 6. (A)The charge separation and transfer in the Co_1Ag_1-PCN DAC system under solar light irradiation. (B) Time course of H_2 production of CN, Ag_1-CN, Co_1-PCN, and 0.1Co_1Ag_1-PCN (C) Wavelength-dependent AQY for photocatalytic H_2 evolution of 0.1Co_1Ag_1-PCN. (D) Recycled H_2 evolution performance of 0.1Co_1Ag_1-PCN. (E) Mott–Schottky plots PDOS plots of (F) Ag 3d for Ag_1-CN, 0.1Co_1Ag_1-PCN, and (G) Co 3d for Co_1-PCN, 0.1Co_1Ag_1-PCN. (H) Differential charge of Co 3d and Ag 3d for 0.1Co_1Ag_1-PCN. (I) Gibbs free energy diagrams and the pathways of HER of Ag_1-CN, Co1-PCN, and 0.1Co_1Ag_1-PCN. Adapted with permission from [30], Copyright 2023 WILEY - V C H VERLAG GMBH & CO. KGAA; Wiley.

Furthermore, (Figure 6I) shows the DFT calculated free energy diagram, suggesting the optimized Gibbs free energy of H* (0.15 eV) for H_2 generation over Co_1Ag_1-PCN compared to the mono SACs. The cooperative interactions between Co and Ag lower the kinetic barrier and facilitate electron accumulation on Ag, thereby enhancing photocatalytic performance.

Preprints (www.preprints.org) | NOT PEER-REVIEWED | Posted: 8 October 2023 doi:10.20944/preprints202310.0446.v1

In summary, this rational design of double-metal SACs creates opportunities to optimize catalytic performance by engineering the atomic coordination environment. The cooperative effects between Co and Ag were successfully established via modulation of charge density and band structures. Further studies on the synthetic control and applications of multi-metallic SACs are expected

4.2. Bimetallic Single-Atom Catalysts Supported on Two-Dimensional Polymerized Carbon Nitride

This paper reports the development of a bimetallic Pt_1-Co_1/CN single-atom catalyst for enhanced photocatalytic hydrogen production. The catalyst is synthesized by dispersing Co single atoms on two-dimensional polymeric carbon nitride (CN) sheets, followed by incorporation of Pt single atoms via a freezing-visible-light-deposition method.

Characterization by EXAFS (Figure 7A) reveals that the Co single atoms in Co1/CN exhibit a Co_1N_4 configuration, while in Pt_1-Co_1/CN the coordination number decreases to Co_1N_3, indicating modulation of the Co sites by Pt. XPS and EPR verify the decrease in Co oxidation state and increase in unpaired electrons in Pt_1-Co_1/CN. Accordingly, Pt_1-Co_1/CN shows dramatically enhanced photocatalytic H2 production (Figure 7B), with rates 19.8 and 3.5 times higher than Co_1/CN and Pt_1/CN respectively. Optical characterization (Figure 7C-F) confirms Pt_1-Co_1/CN has superior visible light response and charge separation. XPS (Figure 7G) verifies the modulation of Co sites by Pt single atoms. DFT calculations (Figure 7H-I) show the Co_1N_3 sites have unpaired 3d electrons crossing the Fermi level, narrowing the bandgap. This unique configuration improves visible light absorption, charge separation, and proton activation.

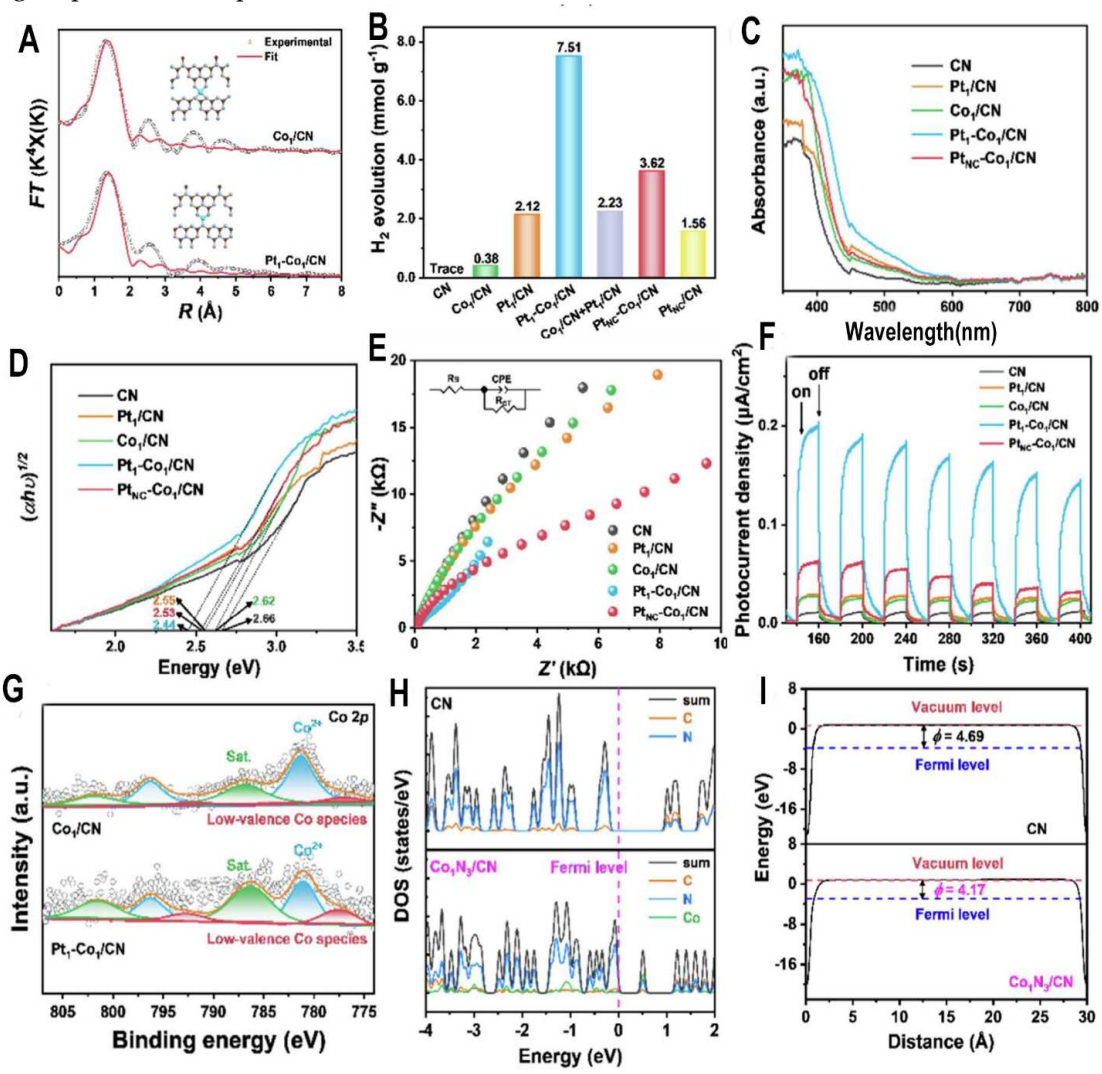

 doi:10.20944/preprints202310.0446.v1

Figure 7. (A) Co K-edge R space EXAFS fitting results of Co_1/CN and Pt1-Co_1/CN samples. Insert are the schematic model of Co_1N_4 sites on Co_1/CN and Co_1N_3 sites on Pt_1-Co_1CN obtained from EXAFS fitting results (B) photocatalytic hydrogen evolution activities of CN, Pt_1/CN, Co_1/CN, Pt_1-Co_1/CN and Pt_{NC}-Co_1/CN samples (C) UV-vis absorption spectra (D) Tauc plots (E) electrochemical impedance spectra (EIS) (F) photocurrent response, (G) Co 2p XPS spectra of Co_1/CN and Pt_1-Co_1/CN samples (H) Projected density of states of CN and Co_1N_3/CN. (I) Work functions of CN and Co_1N_3/CN. Adapted with permission from [74], Copyright 2023 Elsevier B.V.; Elsevier.

In summary, this work demonstrates a synergistic effect between Pt and Co single atoms in CN, where Pt modulates the geometric and electronic configuration of Co. This long-range electron synergy promotes photocatalytic performance by enhancing light absorption, carrier separation, and proton activation. The concept of utilizing bimetallic single atoms and their interactions to tune photocatalyst properties represents an exciting new direction for designing efficient catalysts. Key achievements include maximizing noble metal efficiency, elucidating the electron-level synergistic mechanism, and providing a general strategy to regulate single-atom sites via long-range electron effects. Overall, this work makes important fundamental advances in photocatalysis. The results are significant because they provide critical insights into engineering highly active photocatalysts through precise control and synergistic design of bimetallic single-atom sites. The knowledge gained can guide the continued development of efficient, low-cost photocatalytic systems for renewable energy applications. I find this work highly innovative in exploiting interactions between single atoms to tune catalytic properties.

5. Conclusion and Outlook

This review summarizes recent advances in bimetallic single-atom catalysts for enhanced hydrogen evolution across electrochemical and photocatalytic pathways. Key synergies arise from geometric and electronic modulation of active sites, which were leveraged in systems like W-Mo, Ru-Bi, Ni-Fe, and Pt-Co to optimize hydrogen binding energies, charge transfer properties, and metal-support anchoring. 2D material created stable scaffolds to coordinate isolated dual metal atoms and harness cooperative effects.

Moving forward, several priorities can accelerate progress from fundamental studies to practical applications. Firstly, precision synthetic techniques must continue improving to achieve atomically precise control over compositions and configurations, a key enabler for optimizing activity, selectivity, and stability. Secondly, new techniques like cryo-EM and in situ spectroscopy are needed to provide atomic-scale insights into synergistic mechanisms. Furthermore, extending bimetallic single-atom catalyst design principles to ternary and quaternary systems may uncover new cooperative phenomena toward enhanced hydrogen evolution kinetics. Surface functionalization and semiconductor coupling represent other promising directions for solar-driven hydrogen production Finally, a key challenge lies in translating laboratory-synthesized catalysts into industrial systems. Comparative studies identifying performance gaps can guide scale-up efforts through manufacturing optimizations and process integration.

In summary, this emerging field holds immense potential for enabling clean, efficient hydrogen production. Sustained research into bimetallic single-atom synergies and support interactions, underpinned by advancements in characterization and computation, will accelerate the rational design of optimal catalytic systems.

Funding: This work was financially supported by the Natural Science Foundation of China (51902101, 22202065), the Youth Natural Science Foundation of Hunan Province (2021JJ540044), the Natural Science Foundation of Jiangsu Province (BK20201381), and the Science Foundation of Nanjing University of Posts and Telecommunications (NY219144).

Data Availability Statement: All of the data analyzed in this review came from articles that mentioned studies.

Conflicts of Interest: The authors declare that they have no known competing financial interests or personal relationships that could have appeared to influence the work reported in this paper.

References

1. Turner, J.A. Sustainable Hydrogen Production. Science 2004, 305, 972–974.
2. Jaramillo, T.F.; Jørgensen, K.P.; Bonde, J.; Nielsen, J.H.; Horch, S.; Chorkendorff, I. Identification of Active Edge Sites for Electrochemical H2 Evolution from MoS_2 Nanocatalysts. science 2007, 317, 100–102.
3. Hinnemann, B.; Moses, P.G.; Bonde, J.; Jørgensen, K.P.; Nielsen, J.H.; Horch, S.; Chorkendorff, I.; Nørskov, J.K. Biomimetic Hydrogen Evolution: MoS_2 Nanoparticles as Catalyst for Hydrogen Evolution. J. Am. Chem. Soc. 2005, 127, 5308–5309.
4. Tian, J.; Liu, Q.; Asiri, A.M.; Sun, X. Self-Supported Nanoporous Cobalt Phosphide Nanowire Arrays: An Efficient 3D Hydrogen-Evolving Cathode over the Wide Range of pH 0–14. J. Am. Chem. Soc. 2014, 136, 7587–7590.
5. Carmo, M.; Fritz, D.L.; Mergel, J.; Stolten, D. A Comprehensive Review on PEM Water Electrolysis. Int. J. Hydrog. Energy 2013, 38, 4901–4934.
6. Seh, Z.W.; Kibsgaard, J.; Dickens, C.F.; Chorkendorff, I.; Nørskov, J.K.; Jaramillo, T.F. Combining Theory and Experiment in Electrocatalysis: Insights into Materials Design. Science 2017, 355, eaad4998.
7. Li, Y.; Wei, J.; Cui, N.; Li, J.; Xu, M.; Pan, G.; Jiang, Z.; Cui, X.; Niu, X.; Li, J. Recent Advance of Atomically Dispersed Dual-Metal Sites Carbocatalysts: Properties, Synthetic Materials, Catalytic Mechanisms, and Applications in Persulfate-Based Advanced Oxidation Process. Adv. Funct. Mater. 2023, 2301229.
8. Ren, W.; Cheng, C.; Shao, P.; Luo, X.; Zhang, H.; Wang, S.; Duan, X. Origins of Electron-Transfer Regime in Persulfate-Based Nonradical Oxidation Processes. Environ. Sci. Technol. 2022, 56, 78–97, doi: 10.1021/acs.est.1c05374.
9. Shang, Y.; Xu, X.; Gao, B.; Wang, S.; Duan, X. Single-Atom Catalysis in Advanced Oxidation Processes for Environmental Remediation. Chem. Soc. Rev. 2021, 50, 5281–5322.
10. Yin, K.; Peng, L.; Chen, D.; Liu, S.; Zhang, Y.; Gao, B.; Fu, K.; Shang, Y.; Xu, X. High-Loading of Well Dispersed Single-Atom Catalysts Derived from Fe-Rich Marine Algae for Boosting Fenton-like Reaction: Role Identification of Iron Center and Catalytic Mechanisms. Appl. Catal. B Environ. 2023, 122951.
11. Chen, Y.; Yang, Y.; Ren, N.; Duan, X. Single-Atom Catalysts Derived from Biomass: Low-Cost and High-Performance Persulfate Activators for Water Decontamination. Curr. Opin. Chem. Eng. 2023, 41, 100942.
12. Tiwari, J.N.; Singh, A.N.; Sultan, S.; Kim, K.S. Recent Advancement of P-and d-Block Elements, Single Atoms, and Graphene-Based Photoelectrochemical Electrodes for Water Splitting. Adv. Energy Mater. 2020, 10, 2000280.
13. Li, J.; Yang, Z.; Li, Y.; Zhang, G. Advances in Single-Atom Catalysts: Design, Synthesis and Environmental Applications. J. Hazard. Mater. 2022, 429, 128285, doi: 10.1016/j.jhazmat.2022.128285.
14. Yang, X.-F.; Wang, A.; Qiao, B.; Li, J.; Liu, J.; Zhang, T. Single-Atom Catalysts: A New Frontier in Heterogeneous Catalysis. Acc. Chem. Res. 2013, 46, 1740–1748.
15. Zhang, Y.; Yang, J.; Ge, R.; Zhang, J.; Cairney, J.M.; Li, Y.; Zhu, M.; Li, S.; Li, W. The Effect of Coordination Environment on the Activity and Selectivity of Single-Atom Catalysts. Coord. Chem. Rev. 2022, 461, 214493.
16. Li, L.; Chang, X.; Lin, X.; Zhao, Z.-J.; Gong, J. Theoretical Insights into Single-Atom Catalysts. Chem. Soc. Rev. 2020, 49, 8156–8178.
17. Liu, M.; Wang, L.; Zhao, K.; Shi, S.; Shao, Q.; Zhang, L.; Sun, X.; Zhao, Y.; Zhang, J. Atomically Dispersed Metal Catalysts for the Oxygen Reduction Reaction: Synthesis, Characterization, Reaction Mechanisms, and Electrochemical Energy Applications. Energy Environ. Sci. 2019, 12, 2890–2923.
18. Sarma, B.B.; Maurer, F.; Doronkin, D.E.; Grunwaldt, J.-D. Design of Single-Atom Catalysts and Tracking Their Fate Using Operando and Advanced X-Ray Spectroscopic Tools. Chem. Rev. 2023, 123, 379–444, doi: 10.1021/acs.chemrev.2c00495.
19. Qin, R.; Liu, K.; Wu, Q.; Zheng, N. Surface Coordination Chemistry of Atomically Dispersed Metal Catalysts. Chem. Rev. 2020, 120, 11810–11899, doi: 10.1021/acs.chemrev.0c00094.
20. Yan, H.; Cheng, H.; Yi, H.; Lin, Y.; Yao, T.; Wang, C.; Li, J.; Wei, S.; Lu, J. Single-Atom Pd1/Graphene Catalyst Achieved by Atomic Layer Deposition: Remarkable Performance in Selective Hydrogenation of 1, 3-Butadiene. J. Am. Chem. Soc. 2015, 137, 10484–10487.
21. Wei, Z.; Sun, J.; Li, Y.; Datye, A.K.; Wang, Y. Bimetallic Catalysts for Hydrogen Generation. Chem. Soc. Rev. 2012, 41, 7994–8008.
22. Pu, Z.; Amiinu, I.S.; Cheng, R.; Wang, P.; Zhang, C.; Mu, S.; Zhao, W.; Su, F.; Zhang, G.; Liao, S. Single-Atom Catalysts for Electrochemical Hydrogen Evolution Reaction: Recent Advances and Future Perspectives. Nano-Micro Lett. 2020, 12, 1–29.

23. Zhang, H.; Sun, J.; Dagle, V.L.; Halevi, B.; Datye, A.K.; Wang, Y. Influence of ZnO Facets on Pd/ZnO Catalysts for Methanol Steam Reforming. ACS Catal. 2014, 4, 2379–2386, doi:10.1021/cs500590t.
24. Davidson, S.D.; Zhang, H.; Sun, J.; Wang, Y. Supported Metal Catalysts for Alcohol/Sugar Alcohol Steam Reforming. Dalton Trans. 2014, 43, 11782–11802.
25. Cui, X.; Li, W.; Ryabchuk, P.; Junge, K.; Beller, M. Bridging Homogeneous and Heterogeneous Catalysis by Heterogeneous Single-Metal-Site Catalysts. Nat. Catal. 2018, 1, 385–397.
26. Li, X.; Hao, X.; Abudula, A.; Guan, G. Nanostructured Catalysts for Electrochemical Water Splitting: Current State and Prospects. J. Mater. Chem. A 2016, 4, 11973–12000.
27. Jiang, Y.; Lu, Y. Designing Transition-Metal-Boride-Based Electrocatalysts for Applications in Electrochemical Water Splitting. Nanoscale 2020, 12, 9327–9351.
28. Chen, Z.; Qing, H.; Zhou, K.; Sun, D.; Wu, R. Metal-Organic Framework-Derived Nanocomposites for Electrocatalytic Hydrogen Evolution Reaction. Prog. Mater. Sci. 2020, 108, 100618.
29. Khalafallah, D.; Zhi, M.; Hong, Z. Recent Trends in Synthesis and Investigation of Nickel Phosphide Compound/Hybrid-Based Electrocatalysts Towards Hydrogen Generation from Water Electrocatalysis. Top. Curr. Chem. 2019, 377, 29, doi:10.1007/s41061-019-0254-3.
30. Liu, Y.; Sun, Y.; Zhao, E.; Yang, W.; Lin, J.; Zhong, Q.; Qi, H.; Deng, A.; Yang, S.; Zhang, H. Atomically Dispersed Silver-Cobalt Dual-Metal Sites Synergistically Promoting Photocatalytic Hydrogen Evolution. Adv. Funct. Mater. 2023, 2301840.
31. Yang, Y.; Qian, Y.; Li, H.; Zhang, Z.; Mu, Y.; Do, D.; Zhou, B.; Dong, J.; Yan, W.; Qin, Y. O-Coordinated W-Mo Dual-Atom Catalyst for pH-Universal Electrocatalytic Hydrogen Evolution. Sci. Adv. 2020, 6, eaba6586.
32. Yan, Y.; Wang, C.; Huang, Z.; Fu, J.; Lin, Z.; Zhang, X.; Ma, J.; Shen, J. Highly Efficient and Robust Catalysts for the Hydrogen Evolution Reaction by Surface Nano Engineering of Metallic Glass. J. Mater. Chem. A 2021, 9, 5415–5424, doi:10.1039/D0TA10235K.
33. Liu, R.; Fei, H.-L.; Ye, G.-L. Recent Advances in Single Metal Atom-Doped MoS_2 as Catalysts for Hydrogen Evolution Reaction. Tungsten 2020, 2, 147–161, doi:10.1007/s42864-020-00045-7.
34. Yang, K.; Chen, J.; Mi, J.; Yin, R.; Yuan, J.; Shi, J.; Wang, G.; Li, J. More than Just a Reactant: H_2O Promotes Carbonyl Sulfide Hydrolysis Activity over Ni-MgAl-LDO by Inhibiting H2S Poisoning. Fuel 2023, 333, 126503.
35. Wu, P.; Ding, S.; Shen, K.; Yang, H.; Wang, S.; Zhang, S.; Zhang, Y. Enhanced Performance and DFT Study of Sulfur Poisoning Mechanism of Modified Al2O3 Catalyst in COS Hydrolysis. Fuel 2023, 337, 127163.
36. Xie, Y.; Bao, J.; Song, X.; Sun, X.; Ning, P.; Wang, C.; Wang, F.; Ma, Y.; Fan, M.; Li, K. Catalysts for Gaseous Organic Sulfur Removal. J. Hazard. Mater. 2023, 442, 130029.
37. Rocha, G.F.S.R.; Silva, M.A.R. da; Rogolino, A.; Diab, G.A.A.; Noleto, L.F.G.; Antonietti, M.; Teixeira, I.F. Carbon Nitride Based Materials: More than Just a Support for Single-Atom Catalysis. Chem. Soc. Rev. 2023, 52, 4878–4932, doi:10.1039/D2CS00806H.
38. Chen, Z.; Vorobyeva, E.; Mitchell, S.; Fako, E.; López, N.; Collins, S.M.; Leary, R.K.; Midgley, P.A.; Hauert, R.; Pérez-Ramírez, J. Single-Atom Heterogeneous Catalysts Based on Distinct Carbon Nitride Scaffolds. Natl. Sci. Rev. 2018, 5, 642–652, doi:10.1093/nsr/nwy048.
39. Guo, F.; Li, S.; Hou, Y.; Xu, J.; Lin, S.; Wang, X. Metalated Carbon Nitrides as Base Catalysts for Efficient Catalytic Hydrolysis of Carbonyl Sulfide. Chem. Commun. 2019, 55, 11259–11262, doi:10.1039/C9CC06246G.
40. Wang, L.; Wang, D.; Li, Y. Single-atom Catalysis for Carbon Neutrality. Carbon Energy 2022, 4, 1021–1079, doi:10.1002/cey2.194.
41. Sui, X.; Zhang, L.; Li, J.; Doyle-Davis, K.; Li, R.; Wang, Z.; Sun, X. Advanced Support Materials and Interactions for Atomically Dispersed Noble-Metal Catalysts: From Support Effects to Design Strategies. Adv. Energy Mater. 2022, 12, 2102556, doi:10.1002/aenm.202102556.
42. Loy, A.C.M.; Teng, S.Y.; How, B.S.; Zhang, X.; Cheah, K.W.; Butera, V.; Leong, W.D.; Chin, B.L.F.; Yiin, C.L.; Taylor, M.J. Elucidation of Single Atom Catalysts for Energy and Sustainable Chemical Production: Synthesis, Characterization and Frontier Science. Prog. Energy Combust. Sci. 2023, 96, 101074.
43. Giulimondi, V.; Ruiz–Ferrando, A.; Clark, A.H.; Kaiser, S.K.; Krumeich, F.; Martín, A.J.; López, N.; Pérez–Ramírez, J. Catalytic Synergies in Bimetallic Ru Pt Single–Atom Catalysts via Speciation Control. Adv. Funct. Mater. 2022, 32, 2206513, doi:10.1002/adfm.202206513.

44. Jin, H.; Zhou, K.; Zhang, R.; Cui, H.; Yu, Y.; Cui, P.; Song, W.; Cao, C. Regulating the Electronic Structure through Charge Redistribution in Dense Single-Atom Catalysts for Enhanced Alkene Epoxidation. Nat. Commun. 2023, 14, 2494, doi:10.1038/s41467-023-38310-1.
45. Fu, Z.; Yang, B.; Wu, R. Understanding the Activity of Single-Atom Catalysis from Frontier Orbitals. Phys. Rev. Lett. 2020, 125, 156001, doi:10.1103/PhysRevLett.125.156001.
46. Bimetallic Single-Cluster Catalysts Anchored on Graphdiyne for Alkaline Hydrogen Evolution Reaction Available online: https://www.cjcatal.com/EN/10.1016/S1872-2067%2823%2964459-6 (accessed on 3 October 2023).
47. Wang, W.; Song, Q.; Luo, Q.; Li, L.; Huo, X.; Chen, S.; Li, J.; Li, Y.; Shi, S.; Yuan, Y.; et al. Photothermal-Enabled Single-Atom Catalysts for High-Efficiency Hydrogen Peroxide Photosynthesis from Natural Seawater. Nat. Commun. 2023, 14, 2493, doi:10.1038/s41467-023-38211-3.
48. Zhang, H.; Chhowalla, M.; Liu, Z. 2D Nanomaterials: Graphene and Transition Metal Dichalcogenides. Chem. Soc. Rev. 2018, 47, 3015–3017, doi:10.1039/C8CS90048E.
49. Gmitra, M.; Fabian, J. Graphene on Transition-Metal Dichalcogenides: A Platform for Proximity Spin-Orbit Physics and Optospintronics. Phys. Rev. B 2015, 92, 155403, doi:10.1103/PhysRevB.92.155403.
50. Working-in-Tandem Mechanism of Multi-Dopants in Enhancing Electrocatalytic Nitrogen Reduction Reaction Performance of Carbon-Based Materials | SpringerLink Available online: https://link.springer.com/article/10.1007/s12274-021-3315-1 (accessed on 3 October 2023).
51. Kim, H.S.; Lee, C.H.; Jang, J.-H.; Kang, M.S.; Jin, H.; Lee, K.-S.; Lee, S.U.; Yoo, S.J.; Yoo, W.C. Single-Atom Oxygen Reduction Reaction Electrocatalysts of Fe, Si, and N Co-Doped Carbon with 3D Interconnected Mesoporosity. J. Mater. Chem. A 2021, 9, 4297–4309, doi:10.1039/D0TA11208A.
52. Tian, S.; Tang, Q. Activating Transition Metal Dichalcogenide Monolayers as Efficient Electrocatalysts for the Oxygen Reduction Reaction via Single Atom Doping. J. Mater. Chem. C 2021, 9, 6040–6050, doi:10.1039/D1TC00668A.
53. Ge, J.; Zhang, D.; Qin, Y.; Dou, T.; Jiang, M.; Zhang, F.; Lei, X. Dual-Metallic Single Ru and Ni Atoms Decoration of MoS_2 for High-Efficiency Hydrogen Production. Appl. Catal. B Environ. 2021, 298, 120557.
54. Wang, Q.; Hisatomi, T.; Jia, Q.; Tokudome, H.; Zhong, M.; Wang, C.; Pan, Z.; Takata, T.; Nakabayashi, M.; Shibata, N. Scalable Water Splitting on Particulate Photocatalyst Sheets with a Solar-to-Hydrogen Energy Conversion Efficiency Exceeding 1%. Nat. Mater. 2016, 15, 611–615.
55. Zhao, L.; Han, X.; Kong, W.; Tong, Y.; Ding, Y.; Wang, J.; Li, B.; Liu, Y.; Xu, J.; Xing, W. Graphene Supported Single Metal Atom Catalysts for the Efficient Hydrogen Oxidation Reaction in Alkaline Media. Catal. Sci. Technol. 2022, 12, 530–541, doi:10.1039/D1CY01959G.
56. Zhao, X.; Wu, G.; Zheng, X.; Jiang, P.; Yi, J.; Zhou, H.; Gao, X.; Yu, Z.; Wu, Y. A Double Atomic-Tuned RuBi SAA/Bi@ OG Nanostructure with Optimum Charge Redistribution for Efficient Hydrogen Evolution. Angew. Chem. Int. Ed. 2023, 62, e202300879.
57. Xue, Z.-H.; Luan, D.; Zhang, H.; Lou, X.W.D. Single-Atom Catalysts for Photocatalytic Energy Conversion. Joule 2022.
58. Gao, C.; Low, J.; Long, R.; Kong, T.; Zhu, J.; Xiong, Y. Heterogeneous Single-Atom Photocatalysts: Fundamentals and Applications. Chem. Rev. 2020, 120, 12175–12216, doi: 10.1021/acs.chemrev.9b00840.
59. Hiragond, C.B.; Powar, N.S.; Lee, J.; In, S. Single-Atom Catalysts (SACs) for Photocatalytic CO 2 Reduction with H 2 O: Activity, Product Selectivity, Stability, and Surface Chemistry. Small 2022, 18, 2201428, doi:10.1002/smll.202201428.
60. Niu, Y.; Yue, C.; Li, S.; Che, G.; Su, N.; Dong, H.; Li, C. Recent Advance of Single Atom-Based Photocatalysts for Energy Conversion and Environmental Purification. Carbon Lett. 2023, 33, 957–972, doi:10.1007/s42823-023-00486-3.
61. Zheng, T.; Han, X.; Wang, J.; Xia, Z. Role of Heteroatom-Doping in Enhancing Catalytic Activities and the Stability of Single-Atom Catalysts for Oxygen Reduction and Oxygen Evolution Reactions. Nanoscale 2022, 14, 16286–16294, doi:10.1039/D2NR04880A.
62. Sun, J.-K.; Pan, Y.-W.; Xu, M.-Q.; Sun, L.; Zhang, S.; Deng, W.-Q.; Zhai, D. Heteroatom Doping Regulates the Catalytic Performance of Single-Atom Catalyst Supported on Graphene for ORR. Nano Res. 2023, doi:10.1007/s12274-023-5898-1.
63. Sulfur Vacancy Induced High Performance for Photocatalytic H2 Production over 1T@2H Phase MoS_2 Nanolayers - Catalysis Science & Technology (RSC Publishing) Available online: https://pubs.rsc.org/en/content/articlelanding/2017/cy/c7cy01488k/unauth (accessed on 3 October 2023).

64. Lin, Y.-C.; Chang, Y.-P.; Chen, K.-W.; Lee, T.-T.; Hsiao, B.-J.; Tsai, T.-H.; Yang, Y.-C.; Lin, K.-I.; Suenaga, K.; Chen, C.-H.; et al. Patterning and Doping of Transition Metals in Tungsten Dichalcogenides. Nanoscale 2022, 14, 16968–16977, doi:10.1039/D2NR04677F.
65. Jiang, Z.; Zhou, W.; Hu, C.; Luo, X.; Zeng, W.; Gong, X.; Yang, Y.; Yu, T.; Lei, W.; Yuan, C. Interlayer-Confined NiFe Dual Atoms within MoS_2 Electrocatalyst for Ultra-Efficient Acidic Overall Water Splitting. Adv. Mater. 2023, 2300505.
66. Zheng, X.; Li, P.; Dou, S.; Sun, W.; Pan, H.; Wang, D.; Li, Y. Non-Carbon-Supported Single-Atom Site Catalysts for Electrocatalysis. Energy Environ. Sci. 2021, 14, 2809–2858.
67. Li, W.; Guo, Z.; Yang, J.; Li, Y.; Sun, X.; He, H.; Li, S.; Zhang, J. Advanced Strategies for Stabilizing Single-Atom Catalysts for Energy Storage and Conversion. Electrochem. Energy Rev. 2022, 5, 9, doi:10.1007/s41918-022-00169-z.
68. Zhang, F.; Zhu, Y.; Lin, Q.; Zhang, L.; Zhang, X.; Wang, H. Noble-Metal Single-Atoms in Thermocatalysis, Electrocatalysis, and Photocatalysis. Energy Environ. Sci. 2021, 14, 2954–3009.
69. Single-Atom Catalysts: From Design to Application | Electrochemical Energy Reviews Available online: https://link.springer.com/article/10.1007/s41918-019-00050-6 (accessed on 3 October 2023).
70. Fu, J.; Wang, S.; Wang, Z.; Liu, K.; Li, H.; Liu, H.; Hu, J.; Xu, X.; Li, H.; Liu, M. Graphitic Carbon Nitride Based Single-Atom Photocatalysts. Front. Phys. 2020, 15, 33201, doi:10.1007/s11467-019-0950-z.
71. Recycling Synthesis of Single-Atom Zn-Nitrogen-Carbon Catalyst for Electrocatalytic Reduction of O_2 to H_2O_2 | SpringerLink Available online: https://link.springer.com/article/10.1007/s40843-022-2054-5 (accessed on 3 October 2023).
72. Luo, H.; Liu, Y.; Dimitrov, S.D.; Steier, L.; Guo, S.; Li, X.; Feng, J.; Xie, F.; Fang, Y.; Sapelkin, A.; et al. Pt Single-Atoms Supported on Nitrogen-Doped Carbon Dots for Highly Efficient Photocatalytic Hydrogen Generation. J. Mater. Chem. A 2020, 8, 14690–14696, doi:10.1039/D0TA04431H.
73. Catalysts | Free Full-Text | Graphitic Carbon Nitride Materials for Photocatalytic Hydrogen Production via Water Splitting: A Short Review Available online: https://www.mdpi.com/2073-4344/9/10/805 (accessed on 3 October 2023).
74. Yang, M.; Mei, J.; Ren, Y.; Cui, J.; Liang, S.; Sun, S. Long-Range Electron Synergy over Pt1-Co1/CN Bimetallic Single-Atom Catalyst in Enhancing Charge Separation for Photocatalytic Hydrogen Production. J. Energy Chem. 2023, 81, 502–509.